Finite-size effects in the two-dimensional BCS-BEC crossover

M. Lanaro [1,2] G. Bighin,[1] L. Dell'Anna [1,2,3] and L. Salasnich [1,2,3,4]

[1]*Dipartimento di Fisica e Astronomia "Galileo Galilei", Università di Padova, Via Marzolo 8, I-35131 Padova, Italy*
[2]*Istituto Nazionale di Fisica Nucleare, Sezione di Padova, Via Marzolo 8, I-35131 Padova, Italy*
[3]*Padua QTech Center, University of Padova, Via Gradenigo 6, I-35131 Padova, Italy*
[4]*Istituto Nazione di Ottica del Consiglio Nazionale delle Ricerche, Unita di Sesto Fiorentino, Via Carrara 2, I-50019 Sesto Fiorentino, Italy*

We study the finite-size effects on the BCS-BEC crossover in two dimensions, occurring in confined fermionic superfluids. We analyze several thermodynamic properties, such as the chemical potential, the energy gap, and the superfluid density, taking into account unavoidable quantum fluctuations, and, by means of the renormalization group procedure, we detect the putative Berezinskii-Kosterlitz-Thouless phase transition at finite size.

I. INTRODUCTION

Bose and Fermi superfluids in a lower spatial dimension constitute an extremely active research topic, both theoretically and experimentally. Contrary to the three-dimensional case, mean-field approaches are unreliable in two- and one-dimensional systems and the inclusion of quantum fluctuations is crucial to compare correctly the theoretical predictions with the experimental data and Monte Carlo simulations [1,2].

In two-dimensional (2D) systems the Berezinskii-Kosterlitz-Thouless (BKT) phase transition marks the morphing from a superfluid phase characterized by quasicondensation to a normal phase, in which vortex proliferation destroys progressively the superfluidity [3]. The BKT phase transition has been recently observed experimentally [4–8] in Fermi gases made of alkali-metal atoms, and widely investigated theoretically by several groups [9–14]. However, an accurate study which goes beyond the mean-field level for finite-size systems is still lacking. The study of the role of the confinement for Fermi gases is an experimentally relevant but theoretically challenging problem which requires a significant theoretical effort in order to include finite-size effects and the quantum fluctuations.

In this paper, inspired by the recent experimental achievements of box potentials [15,16], we investigate this puzzling problem studying a 2D Fermi gas in the crossover from the Bardeen-Cooper-Schrieffer (BCS) phase [17] to the Bose-Einstein condensation (BEC) phase [18,19]. First, we will see how, at zero temperature, the energy Δ of the Cooper pairs and the chemical potential μ of the fermionic system change along the BCS-BEC crossover due to the presence of a confining box potential. We also determine the BKT critical temperature by calculating the superfluid fraction and, then, implementing the renormalization group Kosterlitz-Thouless equations [14], we will take into account the finite size of the system [20–22].

II. THEORETICAL FRAMEWORK

We will use the binding energy ϵ_B of Cooper pairs as a tunable interaction parameter along the BCS-BEC crossover.

Remarkably, ϵ_B depends on the ratio μ/Δ by the following simple mean-field formula [23],

$$\frac{\epsilon_B}{\epsilon_F} = 2 \frac{\sqrt{1 + \left(\frac{\mu}{\Delta}\right)^2} - \frac{\mu}{\Delta}}{\sqrt{1 + \left(\frac{\mu}{\Delta}\right)^2} + \frac{\mu}{\Delta}}, \tag{1}$$

where $\epsilon_F = \pi \hbar^2 n/m$ is the 2D Fermi energy of noninteracting two-spin-component fermions with number density n and individual mass m. This expression is a mean-field result which nevertheless works also beyond the mean-field level, including Gaussian fluctuations [13,14]. As shown in Fig. 1, the ratio μ/Δ ranges from $-\infty$, when $\epsilon_B \to +\infty$ (BEC regime), to $+\infty$, when $\epsilon_B \to 0$ (BCS regime). Thus, contrary to the 3D case, in the 2D problem the Cooper pairs always form a bound state. In Fig. 1 we show how the binding energy depends on μ/Δ. The crossover regime (green region) is approximately chosen for μ/Δ in the range $(-1, 1)$ since at $\mu = 0$ the Fermi surface is lost.

Finite-size effects are included through an infrared cutoff k_{min} in the wave number k of the quantum particle of mass m, which corresponds to a wavelength $L = 2\pi/k_{min}$. We are considering the box confinement such that $\epsilon_{min} = \hbar^2 k_{min}/(2m)$ is the lowest single-particle energy of the noninteracting Schrödinger problem. We will analyze the BCS-BEC crossover in two dimensions going beyond the mean-field analysis (both mean-field calculations and details of the beyond-mean-field approach are reported in Appendixes A and B, respectively). The putative Berezinskii-Kosterlitz-Thouless phase transition for finite systems will be obtained by means of the renormalization group (RG) procedure.

III. BEYOND MEAN-FIELD ANALYSIS

The role of fluctuations is crucial in low dimensions. We aim at investigating how some quantities, such as the chemical potential and the energy gap, change in the presence of Gaussian fluctuations. From the gap equation, in the presence
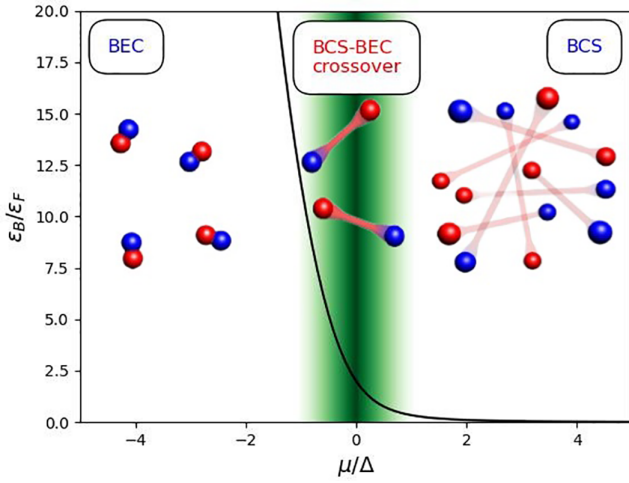
FIG. 1. Binding energy ϵ_B/ϵ_F vs parameter $x_0 = \mu/\Delta$. We show the regions of BCS ($x_0 \to \infty$) and BEC ($x_0 \to -\infty$). The green region points to the relevant values for the BCS-BEC crossover.

of a cutoff, we get (see Appendix B)

$$\Delta = \sqrt{\epsilon_B^2 + 2(\epsilon_{\min} + \mu)\epsilon_B}, \qquad (2)$$

where $\epsilon_{\min} = \hbar^2 k_{\min}^2/(2m)$, and μ is obtained by solving the number equation at the mean-field level supplemented by the Gaussian contribution, $-\frac{d\Omega_{GF}(\mu)}{d\mu}$. Ω_{GF} is the beyond-mean-field grand potential which takes the form

$$\Omega_{GF} = \frac{1}{2\beta} \sum_{\mathbf{q},m} \ln\left[\det \mathbb{M}(\mathbf{q}, i\Omega_m)\right], \qquad (3)$$

where the matrix $\mathbb{M}(\mathbf{q}, i\Omega_m)$ is the inverse pair fluctuation propagator, reported in Appendix B. Following the approach in Ref. [24], we then calculate μ by looking at the maximum of the energy density $E(\mu) = \Omega(\mu) + \mu n$, at a given density n, where $\Omega(\mu) = \Omega_{MF} + \Omega_{GF}$, namely it is composed by the mean-field term and the contribution coming from the Gaussian fluctuations. This procedure for determining the chemical potential beyond the mean-field approach at finite size is computationally demanding and requires a big computational effort [25] and a polynomial fit to smooth the slightly noisy data for the determination of the Berezinskii-Kosterlitz-Thouless critical temperature (see next section). The evaluation of the grand potential in Eq. (3) requires four different integrations: Two of them appear explicitly in Eq. (3), i.e., the momentum integration and the Matsubara frequency sum which can be converted to an integration in the zero-temperature limit, while two are contained in the M matrix elements, i.e., the radial and angular part of the momentum k in Eqs. (B2) and (B3). The two innermost integrations are evaluated using an adaptive algorithm [26], recursively dividing the grid until a certain relative error is required, so in this case we set the maximum relative error to 10^{-5}. The two outermost integrations are performed on a 200×200 grid, using the Gauss-Kronrod quadrature formula. We verify the convergence using a much finer grid for selected data points. In Fig. 2 we plot the energy gap Δ (upper panel)
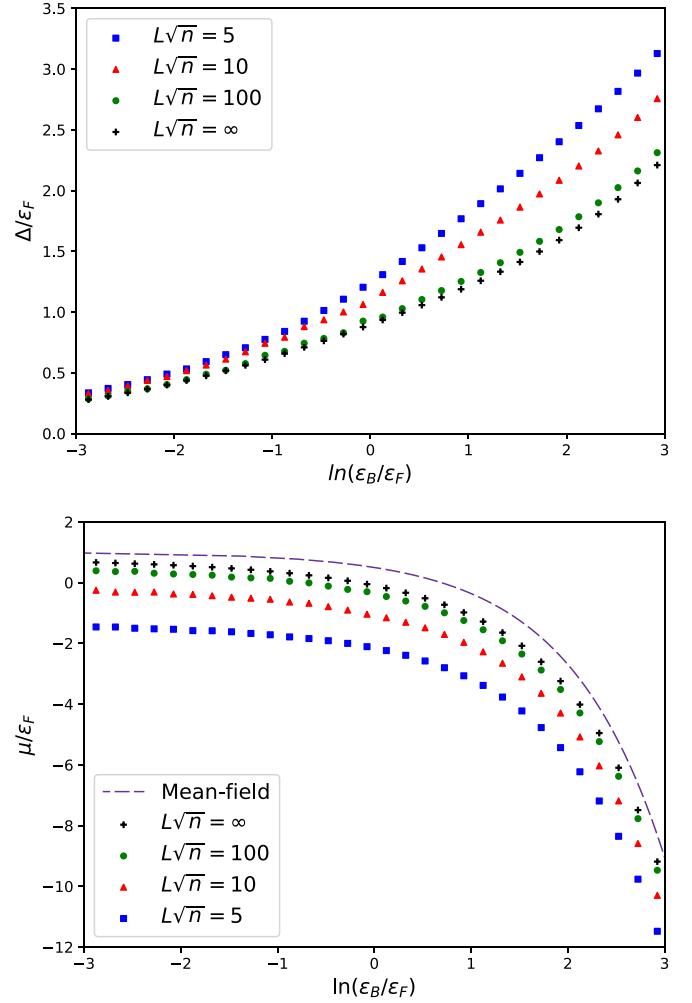

FIG. 2. In the upper panel we show Δ/ϵ_F vs ϵ_B/ϵ_F, while in the lower panel we show μ/ϵ_F vs ϵ_B/ϵ_F for different values of the cutoff, respectively, $L\sqrt{n} = 5$ (blue square points), 10 (red triangle points), 100 (green circular points), and ∞ (black plus points). Here, $L = 2\pi/k_{\min}$ with $k_{\min}$ the infrared cutoff while $\sqrt{n} = 1/d$, with d interparticle distance. In this way, $L\sqrt{n}$ is an adimensional quantity. In the lower panel we have also included the mean-field chemical potential μ which, contrary to the energy gap Δ, is size independent (see Appendix A).

and the chemical potential μ (lower panel) as a function of binding energy.

Finally, let us consider the superfluid density. In order to go beyond the mean-field analysis we have to consider also the collective excitations, so that the superfluid density reads

$$n_s = n - n_{sp} - n_{col}, \qquad (4)$$

where n is the total density, n_{sp} is the mean-field fermionic single-particle contribution to the normal density while n_{col} is the beyond-mean-field contribution coming from the bosonic collective modes

$$n_{col} = \frac{\beta}{2} \int_{k_m}^{\infty} \frac{d^2\mathbf{k}}{(2\pi)^2} \hbar^2 k^2 m \frac{\exp[\beta\mathcal{E}_{col}(\mathbf{k})]}{\{\exp[\beta\mathcal{E}_{col}(\mathbf{k})] - 1\}^2}. \qquad (5)$$

If we make the following ansatz,

$$\mathcal{E}_{col}(\mathbf{k}) \simeq \hbar c_s k, \qquad (6)$$

where c_s is the sound velocity, which in its turn, depends on ϵ_B, we can calculate Eq. (5) and, defining $x_{\min} = \beta \hbar c_s k_{\min}$, we get

$$n_{\text{col}} = \frac{m}{4\pi \hbar^2 c_s^4} \frac{1}{\beta^3} \Big[6 \, \text{Li}_3(e^{x_{\min}}) - 6 x_{\min} \, \text{Li}_2(e^{x_{\min}})$$
$$- x_{\min}^2 \Big(\frac{x \, e^{x_{\min}}}{1 - e^{x_{\min}}} + 3 \ln[1 - e^{x_{\min}}] \Big) \Big]. \tag{7}$$

In the limit $x_{\min} \to 0$, namely for $k_{\min} \to 0$, for an infinite system, only the first term survives and we get

$$n_{\text{col}} = \frac{3m}{2\pi \hbar^2 c_s^4} \frac{\zeta(3)}{\beta^3}, \tag{8}$$

which is the maximum value for n_{col}. We see therefore that the collective excitations further contribute to suppressing the superfluid density. However, such a suppression is less effective for finite-size systems and therefore the superfluid density is expected to be enhanced by finite-size effects.

IV. BEREZINSKII-KOSTERLITZ-THOULESS PHASE TRANSITION

From the Mermin-Wagner-Hohenberg theorem [27,28] we know that in two dimensions the critical temperature at which we have the superconductive phase transition is $T_c = 0$ [29]. However, it is possible to recognize a quasicondensate phase and the temperature under which we can see this type of behavior is called the Berezinskii-Kosterlitz-Thouless temperature (T_{BKT}).

Another important feature characterizing this phase transition is the universal jump of the superfluid density,

$$n_s(T_{\text{BKT}}^-) \neq n_s(T_{\text{BKT}}^+) = 0, \tag{9}$$

that is due to the abrupt unbinding of two vortices that typically describes this transition. Kosterlitz derived a set of renormalized group (RG) equations able to describe the flow of vortices in the two-dimensional Berezinskii-Kosterlitz-Thouless phase transition [30]. The RG equations are the following,

$$\frac{d}{dl} K_l^{-1}(T) = 4\pi^3 y_l^2(T),$$
$$\frac{d}{dl} y_l(T) = [2 - \pi K_l(T)] y_l(T), \tag{10}$$

where $l = \ln(r/d)$, r is the size of the superfluid system, characterized by the presence of vortices, and d can be identified with the interparticle distance.

An important quantity describing the system is the phase stiffness. A fermionic superfluid can be described by the effective Hamiltonian of the two-dimensional XY model, which reads

$$H = \frac{J}{2} \int d^2 \mathbf{r} [\nabla \theta(\mathbf{r})]^2, \tag{11}$$

where the phase stiffness J is a function of the fermion-fermion attractive strength and of the temperature [14]. This quantity is related to the superfluid density via [31]

$$J = \frac{\hbar^2}{4m} n_s, \tag{12}$$

and the superfluid density n_s found through the beyond-mean-field analysis must be computed with the gap energies Δ in the presence of the cutoff. From the phase stiffness, we define then the following quantity,

$$K = \frac{J}{k_B T}. \tag{13}$$

The quantity y, instead, is related to the core vortex energy μ_c such that

$$y = \exp\left[-\frac{\mu_c}{k_B T} \right]. \tag{14}$$

Higher-order terms [32] slightly modify Eq. (10), and therefore can be neglected. In the framework of the two-dimensional XY model the vortex core energy is commonly expressed as $\mu_c = \frac{\pi^2}{4} J$, within the Ginzburg-Landau theory of superconducting films [33]. The starting point for the RG flow is determined by the bare superfluid density, calculated at a fixed temperature T, which defines the initial superfluid stiffness $J_0(T)$. The initial conditions for the RG equations are therefore

$$K_0(T) = \frac{J_0(T)}{k_B T},$$
$$y_0(T) = \exp\left[-\frac{\pi^2}{4} \frac{J_0(T)}{k_B T} \right]. \tag{15}$$

V. SUPERFLUID DENSITY AND CRITICAL TEMPERATURE

We must notice that also the adimensional scaling parameter l of the RG equations will be influenced by the cutoff [20]. The interparticle distance d is taken as the square root of the total density of particles n, i.e., $d = 1/\sqrt{n}$, while L is the size of our system imposed by a confining potential. Therefore, the maximum value of l is

$$l_{\max} = \ln(L/d) = \ln(L\sqrt{n}). \tag{16}$$

In Fig. 3 we show how the inclusion of the cutoff modifies the behavior of n_s/n as a function of T/T_F. The main feature is the disappearance of the universal jump at the critical temperature, replaced by a curve that becomes smoother and smoother upon decreasing the size of the system.

Our aim is now to obtain the critical temperature T_{BKT}/T_F as a function of the normalized binding energy ϵ_B/ϵ_F. In the limit of infinite size, the slope of the tangent of the superfluid density right at the critical temperature goes to infinity. For finite-size systems, instead, the superfluid density is a smooth function. The criterion for identifying the critical temperature, however, can be still based of the maximum value of the slope of the tangent of the superfluid density. The criterion has a certain degree of arbitrariness, therefore we can decide to follow two different procedures. In the first one, we focus on the intersection between the tangent of n_s/n at the inflection point, where the absolute value of the slope is maximum, and the temperature axis, identifying this intersection as the critical temperature for a specific value of ϵ_B/ϵ_F. As shown in Fig. 3, the critical temperatures obtained by this procedure are represented by the triangular points. The slopes are the straight lines and we call these critical
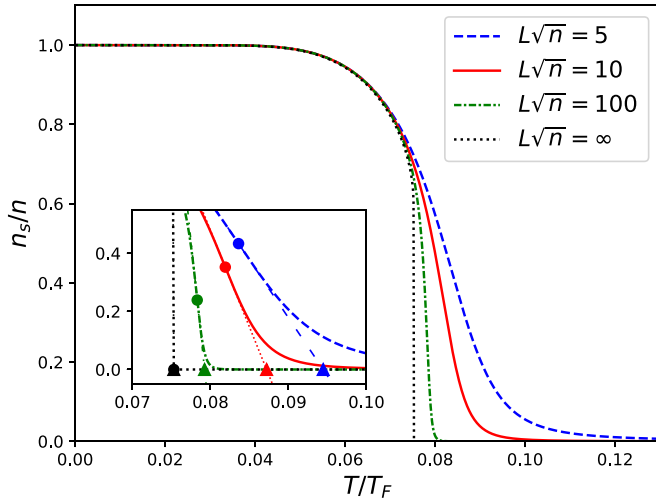
FIG. 3. Main plot: The superfluid density n_s/n vs T/T_F at a fixed value of $\ln(\epsilon_B/\epsilon_F) = 0.92$, for $L\sqrt{n} = 5$ (blue dashed line), 10 (red solid line), 100 (green dashed-dotted line), and ∞ (black dotted line). Inset: Zoom of the main plot. The inflection points of the superfluid density are depicted by circular points while the triangular points are placed at the intersections of the slope at the inflection points with the T axis.

temperatures $(T_{\text{BKT}}/T_F)_{c_1}$. In this way we obtained T_{BKT}/T_F as a function of ϵ_B/ϵ_F for different values of $L\sqrt{n}$, shown in Fig. 4. In the second procedure, also adopted in Ref. [21], we identify the critical temperatures as the x coordinates of the inflection points, where n_s/n has the maximum absolute value of the slope. In Fig. 3 these points are the circular marked ones. The plots of the critical temperature obtained by this latter procedure, called $(T_{\text{BKT}}/T_F)_{c_2}$, as a function of the binding energy, for different values of $L\sqrt{n}$, are showed in Appendix C.
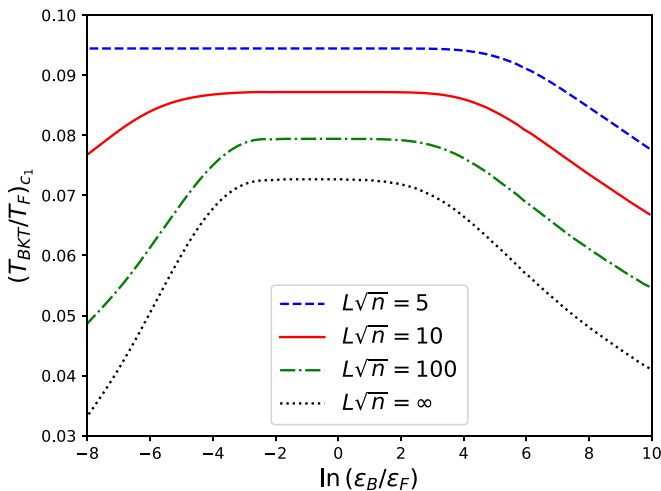

FIG. 4. The critical temperature obtained through the intersection between the tangent to the superfluid density at the inflection point and the horizontal line $n_s/n = 0$ (the triangular points in Fig. 3), i.e., $(T_{\text{BKT}}/T_F)_{c_1}$ against $\ln(\epsilon_B/\epsilon_F)$ (see the main text).

VI. CONCLUSIONS

The main objective of this paper has been to understand how the size of the system, finite in feasible experiments, affects the BCS-BEC crossover in two dimensions. The finite size has been introduced through an infrared cutoff in momentum space. Setting a minimum value to the wave vector corresponds, indeed, to setting a maximum value to the wavelength, which is the size of the system. We have analyzed the effects of the finite size in several thermodynamic properties, such as the chemical potential, the energy gap, and the superfluid density, going beyond the mean-field level by including Gaussian quantum fluctuations. Finally, by means of a renormalization group analysis and defining a couple of criteria useful to identify an effective critical temperature tailored for finite sizes, we have characterized the Berezinskii-Kosterlitz-Thouless phase transition in such systems. We believe that in the near future our theoretical predictions could be compared with the available experimental setups of strongly confined gases of fermionic atoms in quasi-two-dimensional geometry. In particular, the behavior of the measured superfluid density and critical temperature will highlight the reliability and accuracy of the beyond-mean-field theoretical method we have proposed.

APPENDIX A: MEAN-FIELD APPROACH

We will consider in what follows the mean-field analysis. We can start with the bound-state equation of the two-body problem, that, in two dimensions, takes the form

$$-\frac{1}{g} = \frac{1}{\Omega} \sum_{\substack{\mathbf{k} \\ |\mathbf{k}| \geqslant k_{\min}}} \frac{1}{\frac{\hbar^2 k^2}{m} + \epsilon_B}, \tag{A1}$$

where m is the mass of a fermionic particle and Ω is the two-dimensional finite-size volume. The coupling constant g is instead the strength of the attractive potential. At the same

time the gap equation reads

$$-\frac{1}{g} = \frac{1}{\Omega} \sum_{\substack{\mathbf{k} \\ |\mathbf{k}| \geqslant k_{\min}}} \frac{1}{2\sqrt{\left(\frac{\hbar^2 k^2}{2m} - \mu\right)^2 + \Delta^2}}. \qquad (A2)$$

Both Eqs. (A1) and (A2) have ultraviolet divergencies which can be regularized by subtracting one from the other,

$$0 = \sum_{\substack{\mathbf{k} \\ |\mathbf{k}| \geqslant k_{\min}}} \left(\frac{1}{\frac{\hbar^2 k^2}{m} + \epsilon_B} - \frac{1}{2\sqrt{\left(\frac{\hbar^2 k^2}{2m} - \mu\right)^2 + \Delta^2}} \right). \qquad (A3)$$

Working with the two-dimensional continuum limit, $\sum_{\mathbf{k}} \to \frac{\Omega}{(2\pi)^2} \int d^2\mathbf{k} = \frac{\Omega}{2\pi} \int dk\, k$ after some manipulations, we obtain the regularized gap equation in the presence of an infrared cutoff,

$$\epsilon_B = \sqrt{(\epsilon_{\min} - \mu)^2 + \Delta^2} - (\epsilon_{\min} + \mu), \qquad (A4)$$

where the minimum energy is

$$\epsilon_{\min} = \frac{\hbar^2 k_{\min}^2}{2m}. \qquad (A5)$$

We notice that if we impose $\epsilon_{\min} = 0$ we recover the gap equation for an infinite system. The continuum limit (semiclassical approximation) with a cutoff $k_{\min}$ washes out the geometry of the confining box, which is encoded in the discrete energy levels of the single-particle problem. However, the aim of our paper is to show finite-size effects in a quite general framework. We can now express, in the BCS limit, the number of fermionic particles as

$$n = \frac{N}{\Omega} = \frac{2}{\Omega} \sum_{\substack{\mathbf{k} \\ |\mathbf{k}| \geqslant k_{\min}}} \frac{1}{2} \left[1 - \frac{\left(\frac{\hbar^2 k^2}{2m} - \mu\right)}{\sqrt{\left(\frac{\hbar^2 k^2}{2m} - \mu\right)^2 + \Delta^2}} \right]$$

$$= \frac{m}{2\pi \hbar^2} [\sqrt{(\epsilon_{\min} - \mu)^2 + \Delta^2} - \epsilon_{\min} + \mu]. \qquad (A6)$$

If we consider a 2D finite-size system of N fermionic particles of mass m inside a 2D volume Ω and we assume two possible spin states, we have

$$N = 2 \sum_{\substack{\mathbf{k} \\ |\mathbf{k}| \geqslant k_{\min}}} \Theta\left(\tilde{\epsilon}_F - \frac{\hbar^2 k^2}{2m} \right), \qquad (A7)$$

where Θ is the Heaviside function and $\tilde{\epsilon}_F$ is the Fermi energy of noninteracting fermions. The Fermi wave number is related to the Fermi energy by the law $k_F = \sqrt{\frac{2m\tilde{\epsilon}_F}{\hbar^2}}$. From Eq. (A7) we get

$$\tilde{\epsilon}_F = \pi \frac{\hbar^2}{m} n + \epsilon_{\min}. \qquad (A8)$$

As expected, for $\epsilon_{\min} \to 0$ we get the familiar 2D Fermi energy $\tilde{\epsilon}_F = \pi \hbar^2 n/m$ of noninteracting fermions, which is valid in the thermodynamic limit. We rewrite then Eq. (A8) as

$$n = \frac{m}{\hbar^2 \pi} (\tilde{\epsilon}_F - \epsilon_{\min}). \qquad (A9)$$

If we insert the last expression into the left-hand side of (A6) and, after some manipulations, we obtain the following form

for the number equation of a 2D gas,

$$2\tilde{\epsilon}_F = \sqrt{(\epsilon_{\min} - \mu)^2 + \Delta^2} + \epsilon_{\min} + \mu. \qquad (A10)$$

We try to find now an expression for μ and Δ in terms of the binding energy ϵ_B. From Eqs. (A4) and (A10) we get

$$\mu = \tilde{\epsilon}_F - \epsilon_{\min} - \frac{\epsilon_B}{2}. \qquad (A11)$$

From Eq. (A10), and using Eq. (A11) we get

$$\Delta = \sqrt{(2\epsilon_B + 4\epsilon_{\min})(\tilde{\epsilon}_F - \epsilon_{\min})}. \qquad (A12)$$

In both cases, by imposing $\epsilon_{\min} = 0$ we recover the infinite-size results.

In order to have a consistent analysis for different values of $\epsilon_{\min}$ we must look for quantities that are normalized with respect to something that does not depend on $\epsilon_{\min}$ itself. For this reason, we define

$$\epsilon_F \equiv \tilde{\epsilon}_F - \epsilon_{\min}. \qquad (A13)$$

We can then rewrite (A11) and (A12) as

$$\frac{\mu}{\epsilon_F} = 1 - \frac{\epsilon_B}{2\epsilon_F}, \qquad (A14)$$

$$\frac{\Delta}{\epsilon_F} = \sqrt{2\frac{\epsilon_B}{\epsilon_F} + 4\frac{\epsilon_{\min}}{\epsilon_F}}. \qquad (A15)$$

We investigate the behavior of μ/ϵ_F and Δ/ϵ_F at different values of ϵ_B/ϵ_F (see Fig. 5).

As we can see, Δ is influenced by the value of the cutoff. As the cutoff increases, and so the system size decreases, the trend of the function Δ/ϵ_F remains the same, but it moves towards the negative x axis. However, since negative values of the binding energy are not physical, we picture only the first quarter of the Cartesian plane. The chemical potential μ, instead, is not affected by changing the system's size.

Let us now consider the superfluid density. At the mean-field level it takes the following form,

$$n_s = n - n_{\rm sp}, \qquad (A16)$$

where n is the total density and $n_{\rm sp}$ is the single-particle contribution to the normal density. Following the Landau approach [34], $n_{\rm sp}$ can be written as

$$n_{\rm sp} = \beta \int_{k_{\min}}^{\infty} \frac{d^2\mathbf{k}}{(2\pi)^2} \frac{\hbar^2 k^2}{m}$$

$$\times \frac{\exp\left[\beta\sqrt{\left(\frac{\hbar^2 k^2}{2m} - \mu\right)^2 + \Delta^2}\right]}{\left\{\exp\left[\beta\sqrt{\left(\frac{\hbar^2 k^2}{2m} - \mu\right)^2 + \Delta^2}\right] + 1\right\}^2}, \qquad (A17)$$

which, after introducing $\epsilon = \hbar^2 k^2/(2m)$, becomes

$$n_{\rm sp} = \frac{m}{\hbar^2 \pi} \beta \int_{\epsilon_{\min}}^{\infty} d\epsilon\, \epsilon \frac{\exp[\beta\sqrt{(\epsilon - \mu)^2 + \Delta^2}]}{\{\exp[\beta\sqrt{(\epsilon - \mu)^2 + \Delta^2}] + 1\}^2}. \qquad (A18)$$

In the BCS limit, for $\mu > \epsilon_{\min}$ and $\beta \gg 1$, the dependence on the cutoff $\epsilon_{\min}$ is very weak and we can get the

FIG. 6. Critical temperature obtained projecting the inflection points of the superfluid density to the temperature axis (see Fig. 3 of the main text), for $L\sqrt{n} = 5$ (blue dashed line), 10 (red solid line), 100 (green dashed-dotted line), and ∞ (black dotted line).

The matrix $\mathbb{M}(\mathbf{q}, i\Omega_m)$ is the inverse pair fluctuation propagator. It takes the form of a 2×2 matrix, whose elements are

$$
M_{11}(\mathbf{q}, i\Omega_m) = -\frac{1}{g} + \sum_{\substack{\mathbf{k} \\ |\mathbf{k}| \geqslant k_{\min}}} \frac{\tanh(\beta E_{\mathbf{k}}/2)}{2E_{\mathbf{k}}}
$$

$$
\times \left[\frac{(i\Omega_m - E_{\mathbf{k}} + \xi_{\mathbf{k}+\mathbf{q}})(E_{\mathbf{k}} + \xi_{\mathbf{k}})}{(i\Omega_m - E_{\mathbf{k}} + E_{\mathbf{k}+\mathbf{q}})(i\Omega_m - E_{\mathbf{k}} - E_{\mathbf{k}+\mathbf{q}})} \right.
$$

$$
\left. - \frac{(i\Omega_m + E_{\mathbf{k}} + \xi_{\mathbf{k}+\mathbf{q}})(E_{\mathbf{k}} - \xi_{\mathbf{k}})}{(i\Omega_m + E_{\mathbf{k}} - E_{\mathbf{k}+\mathbf{q}})(i\Omega_m + E_{\mathbf{k}} + E_{\mathbf{k}+\mathbf{q}})} \right],
$$
(B2)

$$
M_{12}(\mathbf{q}, i\Omega_m) = -\Delta^2 \sum_{\substack{\mathbf{k} \\ |\mathbf{k}| \geqslant k_{\min}}} \frac{\tanh(\beta E_{\mathbf{k}}/2)}{2E_{\mathbf{k}}}
$$

$$
\times \left[\frac{1}{(i\Omega_m - E_{\mathbf{k}} + E_{\mathbf{k}+\mathbf{q}})(i\Omega_m - E_{\mathbf{k}} - E_{\mathbf{k}+\mathbf{q}})} \right.
$$

$$
\left. + \frac{1}{(i\Omega_m + E_{\mathbf{k}} - E_{\mathbf{k}+\mathbf{q}})(i\Omega_m + E_{\mathbf{k}} + E_{\mathbf{k}+\mathbf{q}})} \right],
$$
(B3)

where $\xi_{\mathbf{k}} = \hbar^2 k^2/(2m) - \mu$ and $E_{\mathbf{k}} = \sqrt{\xi_{\mathbf{k}}^2 + \Delta^2}$. Moreover, the following relations are valid:

$$
M_{11}(\mathbf{q}, -i\Omega_m) = M_{22}(\mathbf{q}, i\Omega_m),
$$
(B4)

$$
M_{12}(\mathbf{q}, -i\Omega_m) = M_{21}(\mathbf{q}, i\Omega_m).
$$
(B5)

The number equation can then be written as

$$
N = \frac{d\Omega}{d\mu} = \frac{\partial \Omega_{\mathrm{MF}}}{\partial \mu} - \frac{\partial \Omega_{\mathrm{GF}}}{\partial \mu} - \frac{\partial \Omega_{\mathrm{GF}}}{\partial \Delta} \frac{\partial \Delta}{\partial \mu}.
$$
(B6)

From (B6) we can get the chemical potential when we are in the presence of the Gaussian fluctuations. We calculate, following Ref. [24], the energy density $E(\mu)$ and we look for
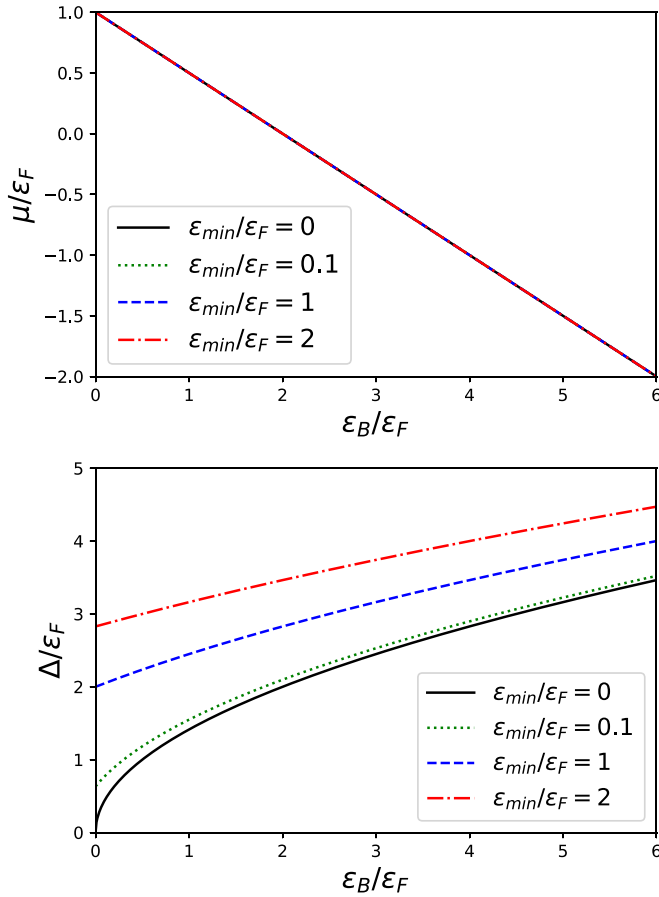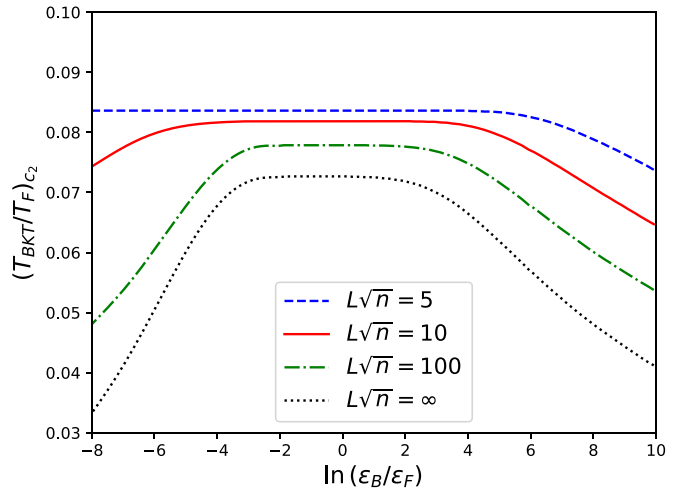
FIG. 5. On the left panel we have μ/ϵ_F vs ϵ_B/ϵ_F for different values of $\epsilon_{\min}/\epsilon_F$, while on the right panel we picture Δ/ϵ_F vs ϵ_B/ϵ_F for different values of $\epsilon_{\min}/\epsilon_F$. In particular, $\epsilon_{\min}/\epsilon_F = 0$ (black solid line), 0.1 (green dotted line), 1 (blue dashed line), and 2 (red dashed-dotted line).

following approximation,

$$
n_{\mathrm{sp}} \approx n \frac{\mu}{\epsilon_F} \sqrt{2\pi \beta \Delta} \exp(-\beta \Delta).
$$
(A19)

The finite-size dependence, in this limit, is therefore mainly due to Δ, which, in the mean-field level, is given by Eq. (A15). Increasing $\epsilon_{\min}$, the gap Δ is enhanced, while n_{sp} is suppressed. As a result, for finite-size systems we expect that the superfluid density is promoted.

APPENDIX B: NUMBER EQUATION WITH INFRARED CUTOFF

The form for the grand potential in the presence of Gaussian fluctuation is $\Omega = \Omega_{\mathrm{MF}} + \Omega_{\mathrm{GF}}$. The first term is the mean-field contribution while the last is due to Gaussian quantum fluctuations which reads

$$
\Omega_{\mathrm{GF}} = \frac{1}{2\beta} \sum_{\mathbf{q}, m} \ln[\det \mathbb{M}(\mathbf{q}, i\Omega_m)].
$$
(B1)

its maximum value that gives the solution of μ for the given density n.

It is important to notice that the momentum integrals we compute in order to get $E(\mu)$ must be done also in the presence of the infrared cutoff in the lower bound. Moreover, in Ref. [24] a dimensionless parameter ν was introduced, which was put in the relation μ and ϵ_B. The presence of the infrared cutoff implies a new definition of ν,

$$\nu = \frac{\mu + \epsilon_B/2 + \epsilon_{\min}}{\epsilon_F}. \tag{B7}$$

This expression allows us indeed to obtain consistent results with the infinite-size case, both for the number and the gap equations.

APPENDIX C: BKT CRITICAL TEMPERATURE

As explained in the main text, we want to compute the critical temperature of the Berezinskii-Kosterlitz-Thouless phase transition. Since in a finite-size system we do not have a universal jump of the superfluid density n_s we decided to propose two different procedures to compute T_{BKT}, based on the inflection points. In the first procedure we identify T_{BKT} as the intersection of the tangent of n_s, as a function of T, at the inflection point with the T axis, for different values of the binding energy ϵ_B (the triangular points in Fig. 3 of the main text). The results obtained by this procedure, $(T_{\text{BKT}/T_F})_{c_1}$, are reported in Fig. 4 of the main text. The second criterion is identifying the critical temperatures just as the projections of the inflection points to the T axis. By this second procedure we obtain the results for T_{BKT}/T_F as functions of the binding energy, $(T_{\text{BKT}}/T_F)_{c_2}$ reported here in Fig. 6.

[1] H. T. C. Stoof, D. B. M. Dickerscheid, and K. Gubbels, *Ultracold Quantum Fields* (Springer, Berlin, 2009).

[2] L. Pitaevskii and S. Stringari, *Bose-Einstein Condensation and Superfluidity* (Oxford University Press, Oxford, U.K., 2016).

[3] *40 Years of Berezinskii-Kosterlitz-Thouless Theory*, edited by J. V. Jose (World Scientific, Singapore, 2013).

[4] Z. Hadzibabic, P. Kruger, M. Cheneau, B. Battelier, and J. Dalibard, Berezinskii-Kosterlitz-Thouless crossover in a trapped atomic gas, Nature (London) **441**, 1118 (2006).

[5] P. Christodoul, M. Gałka, N. Dogra, R. Lopes, J. Schmitt, and Z. Hadzibabic, Observation of first and second sound in a BKT superfluid, Nature (London) **594**, 191 (2021).

[6] P. A. Murthy, I. Boettcher, L. Bayha, M. Holzmann, D. Kedar, M. Neidig, M. G. Ries, A. N. Wenz, G. Zurn, and S. Jochim, Observation of the Berezinskii-Kosterlitz-Thouless phase transition in an ultracold Fermi gas, Phys. Rev. Lett. **115**, 010401 (2015).

[7] I. Boettcher, L. Bayha, D. Kedar, P. A. Murthy, M. Neidig, M. G. Ries, A. N. Wenz, G. Zürn, S. Jochim, and T. Enss, Equation of state of ultracold fermions in the 2D BEC-BCS crossover region, Phys. Rev. Lett. **116**, 045303 (2016).

[8] M. Bohlen, L. Sobirey, N. Luick, H. Biss, T. Enss, T. Lompe, and H. Moritz, Sound propagation and quantum-limited damping in a two-dimensional Fermi gas, Phys. Rev. Lett. **124**, 240403 (2020).

[9] Y.-Y. He, H. Shi, and S. Zhang, Precision Many-Body Study of the Berezinskii-Kosterlitz-Thouless transition and temperature-dependent properties in the two-dimensional Fermi gas, Phys. Rev. Lett. **129**, 076403 (2022).

[10] W. Zhang, G. D. Lin, and L. M. Duan, Berezinskii-Kosterlitz-Thouless transition in a trapped quasi-two-dimensional Fermi gas near a Feshbach resonance, Phys. Rev. A **78**, 043617 (2008).

[11] J. Tempere, S. N. Klimin and J. T. Devreese, The Berezinskii-Kosterlitz-Thouless transition in imbalanced 2D Fermi gases: The role of fluctuations, Physica C: Supercond. **470**, 809 (2010).

[12] S. S. Botelho and C. A. R. Sa de Melo, Vortex-antivortex lattice in ultracold fermionic gases, Phys. Rev. Lett. **96**, 040404 (2006).

[13] G. Bighin and L. Salasnich, Finite-temperature quantum fluctuations in two-dimensional Fermi superfluids, Phys. Rev. B **93**, 014519 (2016).

[14] G. Bighin and L. Salasnich. Vortices and antivortices in two-dimensional ultracold Fermi gases, Sci. Rep. **7**, 45702 (2017).

[15] J. L. Ville, R. Saint-Jalm, E. Le Cerf, M. Aidelsburger, S. Nascimbene, J. Dalibard, and J. Beugnon, Phys. Rev. Lett. **121**, 145301 (2018).

[16] N. Navon, R. P. Smith, and Z. Hadzibabic, Quantum gases in optical boxes, Nat. Phys. **17**, 1334 (2021).

[17] J. Bardeen, L. N. Cooper, and J. R. Schrieffer, Microscopic theory of superconductivity, Phys. Rev. **106**, 162 (1957).

[18] S. Bose, Plancks gesetz und lichtquantenhypothese, Z. Phys. **26**, 178 (1924).

[19] A. Einstein, Quantum theory of the monatomic ideal gas, Sitzungsber. Preuss. Akad. Wiss., Phys.-Math. Kl. 261 (1924).

[20] L. Benfatto, C. Castellani, and T. Giamarchi, Broadening of the Berezinskii-Kosterlitz-Thouless superconducting transition by inhomogeneity and finite-size effects, Phys. Rev. B **80**, 214506 (2009).

[21] A. Tononi, A. Pelster, and L. Salasnich, Topological superfluid transition in bubble-trapped condensates, Phys. Rev. Res. **4**, 013122 (2022).

[22] K. Furutani, A. Perali, and L. Salasnich, Berezinskii-Kosterlitz-Thouless phase transition with Rabi-coupled bosons, Phys. Rev. A **107**, L041302 (2023).

[23] M. Marini, F. Pistolesi, and G. C. Strinati, Evolution from BCS superconductivity to Bose condensation: Analytic results for the crossover in three dimensions, Eur. Phys. J. B **1**, 151 (1998).

[24] L. He, H. Lu, G. Cao, H. Hu, and X.-J. Liu, Quantum fluctuations in the BCS-BEC crossover of two-dimensional Fermi gases, Phys. Rev. A **92**, 023620 (2015).

[25] CloudVeneto is an OpenStack-based cloud managed by University of Padova and INFN, Sezione di Padova and Legnaro National Laboratories.

[26] http://ab-initio.mit.edu/wiki/index.php/Cubature_(Multi-dimensional_integration).

[27] P. C. Hohenberg, Existence of long-range order in one and two dimensions, Phys. Rev. **158**, 383 (1967).

[28] N. D. Mermin and H. Wagner, Absence of ferromagnetism or antiferromagnetism in one-or two-dimensional isotropic Heisenberg models, Phys. Rev. Lett. **17**, 1133 (1966).

[29] A. Altland and B. Simons, *Condensed Matter Field Theory* (Cambridge University Press, Cambridge, U.K., 2010).

[30] J. M. Kosterlitz, The critical properties of the two-dimensional XY model, J. Phys. C: Solid State Phys. **7**, 1046 (1974).

[31] M. E. Fisher, M. N. Barber, and J. Jasnow, Helicity modulus, superfluidity, and scaling in isotropic systems, Phys. Rev. A **8**, 1111 (1973).

[32] D. Amit, *Field Theory, the Renormalization Group, and Critical Phenomena* (World Scientific, Singapore, 1984).

[33] P. Minnhagen and M. Nylén, Charge density of a vortex in the Coulomb-gas analogy of superconducting films, Phys. Rev. B **31**, 5768 (1985).

[34] L. D. Landau, The theory of superfluidity of helium II, J. Phys. USSR **5**, 71 (1941).